Journal of Virological Methods 255 (2018) 14–22

Contents lists available at ScienceDirect

Journal of Virological Methods

journal homepage: www.elsevier.com/locate/jviromet

Differences in the internalization of self-inactivating VSVG-pseudotyped murine leukemia virus-based vectors in human and murine cells

Mónica Loreto Acevedo[a,*], Francisco García-de Gracia[a], Camila Miranda-Cárdenas[a], Ricardo Soto-Rifo[a], Francisco Aguayo[b], Oscar León[a]

[a] Programa de Virología, Instituto de Ciencias Biomédicas, Facultad de Medicina, Universidad de Chile, Chile
[b] Department of Basic and Clinical Oncology, Facultad de Medicina, Universidad de Chile, Santiago, Chile

ARTICLE INFO

Keywords:
VSVG-pseudotyped-MLV
Vector transduction
Reverse transcription
Viral internalization

ABSTRACT

Self-inactivating VSVG-pseudotyped murine leukemia virus (SIN-VSVG-MLV) has been widely used to generate stable cell lines and produce gene delivery vectors. Despite the broad cellular tropism of the VSVG-pseudotyped MLV, we observed differential viral transduction efficiency depending on the host cell type used. In order to determine the mechanism underlying these differences, we used a GFP-expressing SIN-VSVG-MLV and analyzed the major steps of viral transduction in different cell lines including human epithelial, T-lymphocytes, monocytes and murine fibroblast cells.

We observed the better transduction efficiency in HeLa cells, which was 20-fold higher than THP-1 and NIH/3T3 cells. To quantify viral internalization, we determined genomic RNA content by quantifying the early reverse transcription product. Genomic RNA and transduction levels were correlated with HeLa cells showing the higher amount of early RT product followed by tsA201 cells, while NIH/3T3, Jurkat and THP-1 had the lowest amounts. Similar results were observed when the late reverse transcription product was analyzed. Reverse transcription efficiency was 66–85% in HeLa cells and about 30% in tsA201, NIH/3T3, Jurkat and THP-1 cells. Viral integration, determined by Alu-Nested-qPCR, was higher for HeLa and lowerst for Jurkat and THP-1 cells. Interestingly, we observed that viral entry was correlated with the cellular availability of clathrin-mediated endocytosis, which was higher in HeLa and tsA201 cells, potentially explaining the higher rates of SIN-VSVG-MLV transduction and early RT synthesis observed in these cell lines.

In conclusion, the SIN-VSVG-MLV vector showed significantly different rates of infectivity depending on the host cell type, possibly due to differential rates of viral internalization.

1. Introduction

Murine leukemia virus (MLV) is a gammaretrovirus of the *Retroviridae* family. MLV has recently been adopted for use in gene therapy (Hacein-Bey-Abina et al., 2014). MLV vectors are self-inactivating (SIN-MLV) due to a deletion of the U3 region at the 3′ long terminal repeat (LTR) that suppresses the promoter/enhancer activity of the provirus (Hacein-Bey-Abina et al., 2014). In addition, the cloned genes have an internal promoter, which improves vector safety (Cavazza et al., 2013; Schambach et al., 2006; Thornhill et al., 2008).

SIN-MLV vectors can be modified to target specific cell types through pseudotyping, in which the wild-type envelope glycoprotein (Env) is replaced with the envelope of another virus. The vesicular stomatitis virus glycoprotein (VSVG) is often chosen for this application in lentiviruses and SIN-MLV vectors. This glycoprotein uses the low-density lipoprotein (LDL) receptor, located in clathrin-coated pits and caveolae. LDL receptor family members are ubiquitously expressed in many human cell types as well as in mice, chickens, rabbits and other species (Duvillard et al., 2003; Finkelshtein et al., 2013; Ivaturi et al., 2014; Willnow, 1999). Therefore, SIN-VSVG-MLV vectors are useful for transducing a broad range of dividing cells.

The SIN-VSVG-MLV replicative cycle begins after virus entry into the host cell. Upon viral internalization, the single-stranded viral RNA genome is reverse-transcribed to double-stranded DNA by the reverse transcription complex (RTC), which subsequently matures into the pre-integration complex (PIC), which is then transported to the nucleus. During mitosis, the PIC is tethered to the host chromatin by the viral protein p12 (Elis et al., 2012; Schneider et al., 2013), and the viral DNA is integrated into the host DNA by the viral integrase (Craigie et al., 1991). Transduction efficiency depends on many elements, including

* Corresponding author.
E-mail addresses: macevedo@med.uchile.cl (M.L. Acevedo), franciscogarcia96@gmail.com (F. García-de Gracia), camila.miranda.c@gmail.com (C. Miranda-Cárdenas), rsotorifo@uchile.cl (R. Soto-Rifo), faguayo@med.uchile.cl (F. Aguayo), oleon@med.uchile.cl (O. León).

https://doi.org/10.1016/j.jviromet.2018.02.005
Received 19 December 2017; Received in revised form 31 January 2018; Accepted 4 February 2018
Available online 06 February 2018

virus-receptor interactions, entry, reverse transcription, pre-integration complex formation, cell trafficking, nuclear entry, integration and gene expression. The efficiency of these processes often varies depending on the cell type and thus, the type of host cell frequently affects the viral replicative cycle. The RTC and PIC mediate critical early steps in the process and thus, they are sensitive to cell components that may favor or depress replication. For instance, it has been reported that mutagenized HeLa cells may block HIV-1 infection in steps prior to reverse transcription (RT), retarding the synthesis of vDNA and blocking nuclear import of the PIC (Lech and Somia, 2007). Mutagenized CHO-K1 cells have been shown to block MLV infection before or after RT as well as nuclear localization or integration of the vDNA (Bruce et al., 2005). Therefore, the cell type has a physiological effect on the host-virus interaction (Hare et al., 2016). Previous studies using pseudotyped viruses and vectors revealed that MLV pseudotyped with GalV is less infective when produced in A549 cells than when produced in HT-1080 cells. However, replication levels were similar in both cell types during the early steps of infection. The block seemed to occur in A549 cells between RT and integration, likely due to a cell type-dependent restriction of MLV infection resulting from impaired nuclear translocation of the PIC. VSVG glycoprotein incorporation onto the virus surface was sufficient to fully restore the infectivity of A549-produced MLV (Serhan et al., 2002). However, despite the high transduction efficiency and wide tropism of vectors with pseudotyped VSVG, the differences in the replication kinetics in cells of different origins have not been investigated extensively.

Several techniques have been used to monitor the various stages of retroviral replication (Butler et al., 2001; Peng et al., 2014; Schweitzer et al., 2013). Endogenous RT activity has been analyzed by amplifying the strong-stop vDNA or early reverse transcription (ERT) product, which is the first product of reverse transcription, corresponding to a 145-nucleotide region from the 5′ cap of the viral RNA genome covalently linked to the 3′ OH end of the primer $tRNA^{Pro}$ (Van Beveren et al., 1980). The $tRNA^{Pro}$ is later dissociated, hybridizing at the 3′ end and continuing the vDNA synthesis toward the 5′ end. The last region to be retrotranscribed is the Gag ORF, during late reverse transcription (LRT). Cellular factors do not affect the synthesis of strong-stop DNA but do influence LRT synthesis (Warrilow et al., 2010), likely because most cellular factors needed for ERT synthesis are capable of entering the viral core (Santos et al., 2012). Therefore, ERT product levels may provide a good indication of intracellular viral genomic RNA levels.

To determine the dynamics of SIN-VSVG-MLV transduction in different cell lines, we analyzed and compared transduction efficiency, ERT and LRT product levels and viral integration in human adherent epithelial cells (HeLa and tsA201), human suspension cells (T-lymphocytes and monocytes) and, as a host control, murine fibroblast cells (NIH/3T3). We observed differential SIN-VSVG-MLV transduction efficiency depending on the cell type, likely due to differences in vector entry into the various cells analyzed and to a lesser extent, the RT efficiency.

2. Materials and methods

2.1. Cell culture

tsA201 (ECACC-96121229), HeLa (ECACC-93021013) and NIH/3T3 (ATCC CRL-1658) cells were maintained in Dulbecco's modified Eagle's medium (DMEM) supplemented with 10% inactivated fetal bovine serum (HyClone), 8 mM L-glutamine, 100 U/mL penicillin and 100 µg/mL streptomycin. Jurkat E6.1 (ATCC TIB-202) and THP-1 (ECACC 88042803) cells were maintained in RPMI-1640 medium supplemented with 10% inactivated fetal bovine serum (HyClone), 100 U/mL penicillin and 100 µg/mL streptomycin. For THP-1 cells only, 0.05 mM 2-mercaptoethanol was added. All cells were grown in a humidified atmosphere with 5% CO_2 at 37 °C.

2.2. Virus production and titer measurement

Self-inactivating VSVG-pseudotyped MLV-based vector (SIN-VSVG-MLV) was produced by transient triple transfection of tsA201 cells using polyethylenimine (PEI) with pVSVG envelope, pTG5349 packaging plasmid and pRetroQ transfer plasmid in a 1:2:3 ratio. Cell supernatant was collected by centrifugation 48 h after transfection and filtered, and the virus was concentrated as previously described by Kohno et al. (2002), with some modifications. Briefly, 20% polyethylene glycol 10,000 and 1.8% NaCl were mixed with supernatant containing the virus in a 1:1 ratio and incubated for 16 h at 4 °C. The mixture was then centrifuged at 4000 × *g* for 30 min at 4 °C, and the pellet was suspended in DMEM and stored at −80 °C. Viral titer was determined for the GFP signal of plasmid packaging by flow cytometry (FACS) and represented as transduction units, as described by Tiscornia et al. (2006).

2.3. Infection

5×10^5 cells/well of tsA201, 6×10^5/wells of HeLa and 1×10^5/wells of NIH/3T3, Jurkat and THP-1 cells were seeded in a 6-well plate 24 h prior to infection. Cells were transduced at a multiplicity of infection (MOI) of 2 or 5.

2.4. Viral DNA (vDNA) quantification

Transduced cells were washed twice with Buffer A (10 mM Tris-HCl (pH: 7.4); 150 mM KCl; 5 mM $MgCl_2$). Subsequently, cells were incubated for 10 min with gentle agitation at room temperature with 5 volumes of Buffer B (10 mM Tris-HCl, pH: 7.4); 150 mM KCl; 5 mM $MgCl_2$, 1 mM DTT; 1X Protease Inhibitor Cocktail (Roche); 0.025% (w/v) digitonin. Nuclei were pelleted by centrifugation at 1500X *g* for 4 min, and the supernatant was clarified by centrifugation at 19,000 × *g* for 1 min. The supernatant, corresponding to the cytoplasmic extract, was digested for 30 min with 20 µg/ml RNase A (Qiagen). Viral DNA was isolated from lysates using a PureLink PCR Purification Kit (Invitrogen) according to the manufacturer's protocol. Cytoplasmic viral DNA was analyzed by real-time PCR containing 1X Brilliant II SYBR® Green (Agilent), 250 nM primer and 2 µL DNA sample. The primers used to detect the early reverse transcription (ERT) or strong-stop product were 551–568 (5′-TCT TCC GAT AGA CTG CGT-3′) and 651-670 (5′-TGG GTA GTC AAT CAC TCA GA-3′), and the primers used to detect late reverse transcription (LRT) product were 1346-1325 (5′-TGATCTTAACCTGGGTGATGAG-3′) and 1211-1229 (5′-ATCG CTCACAACCAGTCGG-3′); numbers correspond to the regions of the pRetroQ plasmid synthesized at the beginning (ERT) or end (LRT) of reverse transcription. The human mitochondrial primers MH-533 (5′-ACC CAC TCC CTC TTA GCC AAT ATT -3′) and MH-534(5′-GTA GGG CTA GGC CCA CCG-3′), which amplify subunit 4L of NADH dehydrogenase, were used for normalization of cytoplasmic DNA extraction. Primers used to amplify murine mtDNA were as follows: 18S-1546 (5′-TAG AGG GAC AAG TGG CGT TC-3′) and 18S-1650 (5′-CGC TGA GCC AGT CAG TGT-3′). The amplification efficiency of the ERT, LRT and mitochondrial calibrator primers were equal, calibrating by maintaining a constant value of ΔCt (Ct target gene - Ct reference gene) in serial dilution. Real-time PCR was performed using Rotor Gene 6000 (Corbett Research) with the following amplification parameters: initial denaturation at 95 °C for 15 min and 50 cycles of denaturation at 95 °C for 20 s, annealing at 55 °C for 20 s and elongation at 72 °C for 30 s. Fluorescence data were collected during the 72 °C step. The $2_t^{-\Delta\Delta C}$ method was used for relative quantification of vDNA, according to the formula described by Livak and Schmittgen (2001).

2.5. Integration detection

Virus integration was analyzed at different intervals after

transduction. The infected cells were lysed with lysis buffer (10 mM Tris-HCl (pH: 8.5); 5 mM EDTA; 200 mM NaCl; 0.2% SDS; 0.5 mg/mL Proteinase K) for 1 h at 60 °C. Subsequently, 0.4 vol of 4M NaCl was added, and the mixture was incubated on ice for 5 min and then pelleted at maximum speed for 15 min. The supernatant was mixed with 1 vol of isopropanol, and the DNA was precipitated by centrifugation at maximum speed for 10 min. The pellet was washed twice with 70% cold ethanol and resuspended in water. The resulting cellular DNA was subjected to real-time PCR as described by Brussel and Sonigo (2003), with some modifications. In the first round of PCR, we used the Alu1 (5′-TCCCAGCTACTGGGGAGGCTGAGG-3′), Alu2 (5′ GCCTCCCAAAGT GCTGGGATTACAG-3′) and λT LTR1-(5′-ATGCCACGTAAGCGAAACTC CAGTCCTCCGATTGACTGAGT-3′) primers, the last containing a specific phage lambda sequence. For the second round of real-time PCR, the reaction contained 1X HOT FIREPol EvaGreen (Solis BioDyne) and 250 nM primer. The primers were a specific starter phage lambda (λT2: 5′-ATGCCACGTAAGCGAAACT -3′) and a primer with the specific sequence of the LTR (LTR2: 5′-GAAAGACCCCCGCTGACG-3′).

2.6. LDL receptor quantification

4×10^5 HeLa, tsA201, NIH/3T3, Jurkat and THP-1 cells were blocked with PBS and BSA 0,5% for 20 min, then the LDL receptors antibody (Abcam ab52818) diluted 1:1000 was added for 30 min. Cells were washed twice with PBS and the secondary anti-rabbit Alexa488 (Thermofisher R37116) antibody diluted at 1:200 was added for 30 min and washed again. The pellet was suspended in FACS flow medium and analyzed in a BD FACSCalibur Flow Cytometry System.

2.7. Uptake assay

The uptake of fluorescently tagged transferrin was analyzed as described by Kirchhausen (Kirchhausen et al., 2008). Briefly, HeLa, tsA201 and NIH/3T3 cell lines were seeded on coverslips to 75–80% confluence and 10^5 cells/well. Jurkat and THP-1 cells were seeded in a 24-well plate. Cells were washed 4 times with 1X PBS and incubated with 20 μM chlorpromazine (CPZ) inhibitor for 1 h at suitable temperature. Then cells were washed twice with 1X PBS and incubated with 5 μg/mL Transferrin Alexa Fluor 633 (Tf) (Life Technologies) for 15 min. The Jurkat and THP-1 cells were attached to coverslips with poly-lysine. Next, all cells were washed with cold PBS to remove non-specifically bound conjugates. Cells were fixed with 3.7% PFA and sucrose for 30 min, washed with 0.1 M glycine 5% BSA for 1 h and the nucleus stained with 16.2 μM Hoechst for 10 min. Coverslips were mounted with Fluoromount™ Aqueous Mounting medium (Sigma-Aldrich). Cells were observed with a C2 plus confocal microscope. The corrected total cell fluorescence (CTCF) was obtained using the ImageJ software by calculating the mean of fluorescence per the same area for all cell lines analyzed and corrected with the background of each image, the average was calculated by measuring 5 different points.

2.8. Inhibition treatment and viral infection assays

Cell lines were seeded in 24-well plates at a confluence of 80–90%. Cells were washed once with 1x PBS and incubated with 10 μM chlorpromazine (CPZ) (Sigma Aldrich) inhibitor for 1 h at room temperature in the corresponding medium supplemented with 10% FBS. Cells were then transduced with SIN-VSVG-MLV at a MOI of 5 for 48 h. Next, cells were washed with cold PBS and fixed with 2% formaldehyde. Finally, the cells were washed twice with PBS and collected using 100 μL 0.25% trypsin-EDTA and centrifuged at 6000 rpm. The pellet was suspended in FACS flow medium and analyzed in a FACS system.

2.9. Statistical analysis

Statistical analysis were performed using the ANOVA test with the Open Office software. A p-value < 0.05 was considered statistically significant.

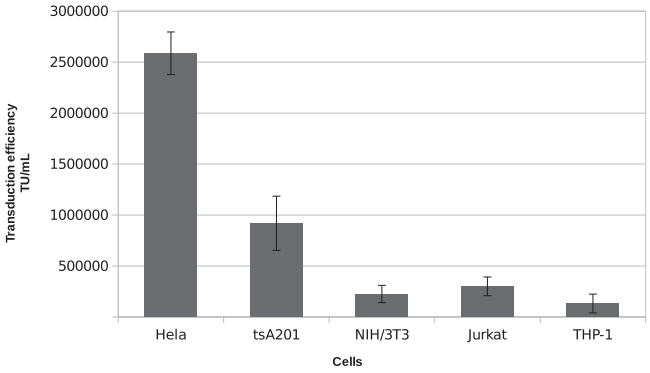

Fig. 1. SIN-VSVG-MLV transduction efficiency in different cell lines. The transduction efficiency of SIN-VSVG-MLV was evaluated in HeLa, NIH/3T3, Jurkat and THP-1 cells by infecting each cell line with an MLV preparation initially titered on tsA201 cells. The titer was determined for each cell line at 3 days, in triplicate. The graphs represent the average viral titer as transduction units (TU) x mL, and the bars show the standard deviation.

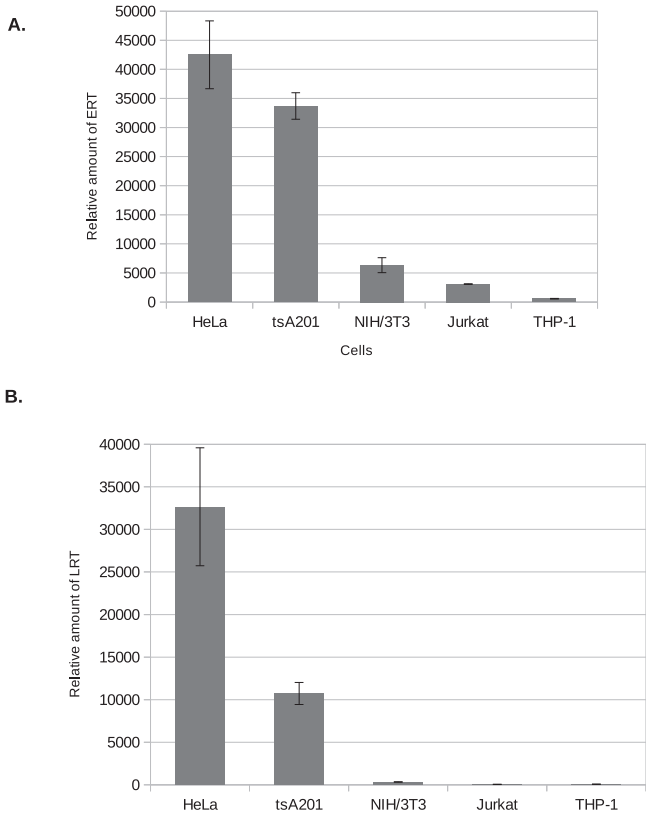

Fig. 2. Quantification of early and late reverse transcription product. HeLa, tsA201, NIH/3T3, Jurkat and THP-1 cells were infected with SIN-VSVG-MLV, and total cytoplasmic DNA was purified and measured with quantitative PCR. The relative amounts of early (A) and late (B) reverse transcription product are shown in the graphs. Each graph represents the average of three independent experiments.

3. Results

3.1. Transduction efficiency of SIN-VSVG-MLV varies between different cell lines

We first sought to determine whether the cell type influenced the efficiency of transduction of SIN-VSVG-MLV. For this, we determined infectious titers from HeLa, tsA201, Jurkat, THP-1 and NIH/3T3 cells.

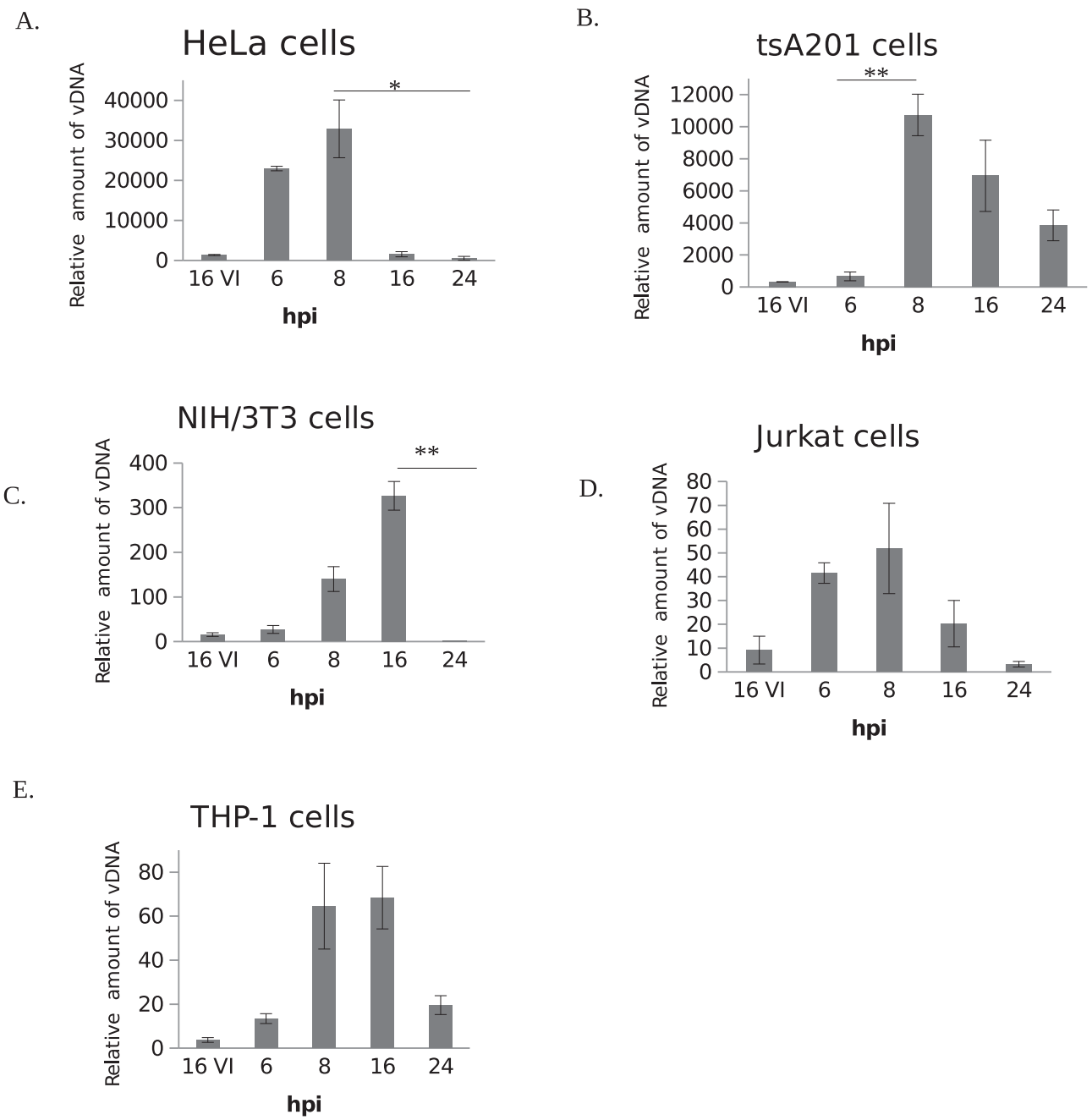

Fig. 3. Viral DNA synthesis. HeLa (A), tsA201 (B) NIH/3T3 (C), Jurkat (D) and THP-1 (E) cells were infected with SIN-VSVG-MLV at different intervals post-infection, and the vDNA or late reverse transcription product was measured with quantitative PCR. Inactivated virus (IV) at 65 °C for 30 min was used as a control. Each graph represents the average of three independent experiments and the bars indicate the standard (*:$p < 0.05$; **: $p < 0.01$; ***:$p < 0.001$).

We used a standard preparation of SIN-VSVG-MLV, previously titered on tsA201 cells, for infection of each cell line and the transduction units (TU) were analyzed on the same amounts of cells. The titers obtained were 9.2×10^5 TU/ml in tsA201 cells; 2.6 (+/− 0.2) $\times 10^6$ TU/ml in HeLa cells; 1.5 (+/− 0.8) $\times 10^5$ TU/ml in NIH/3T3 cells; 3.0 (+/− 0.9) $\times 10^5$ TU/ml in Jurkat cells and 1.3 (+/− 0.9) $\times 10^5$ TU/ml in THP-1 cells. These results show that the transduction efficiency of the SIN-VSVG-MLV vector was approximately 3-fold higher in HeLa cells compared to tsA201 cells. Transduction efficiency was relatively poor in THP-1, Jurkat and NIH/3T3 cells, at levels approximately 3- to 6-fold lower than in tsA201 cells and 17-fold lower than in HeLa cells (Fig. 1).

3.2. SIN-VSVG-MLV vectors produce large amounts of early reverse transcription product in HeLa and tsA201 cells

From data obtained above, it seems that HeLa and tsA201 cells are highly transduced by the SIN-VSVG-MLV vector when compared to Jurkat, THP-1 and NIH/3t3 cells. Thus, we sought to determine which was the step of the replication cycle that was influencing such a difference. To evaluate the rate of RT, we measured the early reverse transcription (ERT) product, also called negative-strand or strong-stop DNA. This first RT product can be synthesized under conditions of limiting substrate concentration (Van Beveren et al., 1980) and without cellular cofactors (Santos et al., 2012; Warrilow et al., 2010). Therefore, the ERT product represents the amount of genomic viral RNA internalized into the cells. We also quantified the late reverse transcription

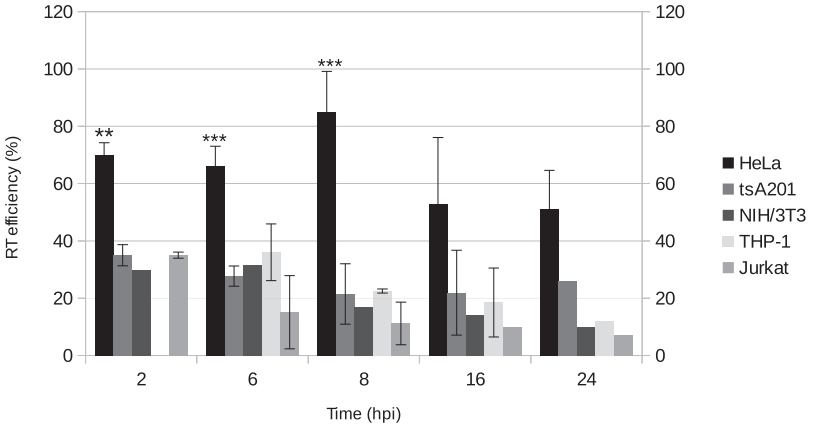

Fig. 4. Reverse transcription efficiency. HeLa, tsA201, NIH/3T3, Jurkat and THP-1 cells were infected with SIN-VSVG-MLV at different intervals post-infection, and reverse transcription efficiency was evaluated by quantification of early (strong-stop) and late reverse transcription product with real-time PCR. The graphs show the average amount of late reverse transcription product relative to strong-stop product, and the bars indicate the standard deviation (**: $p < 0.01$ and ***: $p < 0.001$).

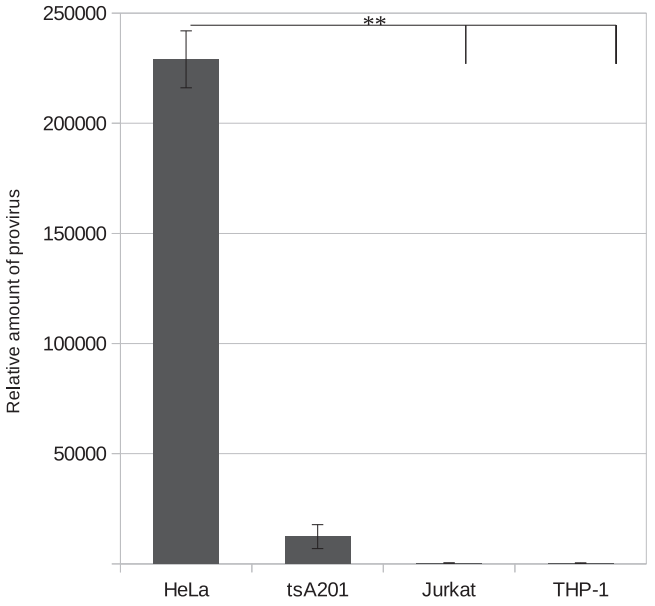

Fig. 5. Integration efficiency. SIN-VSVG-MLV integration was analyzed in HeLa, tsA201, Jurkat and THP-1 cells. The provirus was quantified by two-step *Alu*-based nested PCR assay, and the peak relative quantity of provirus observed was graphed on a linear scale. The bars indicate the standard deviation (**:$p < 0.01$).

(LRT) product, defined as the final vDNA product of RT, which is highly dependent on the RTC formed by viral and cell factors.

To compare ERT and LRT product synthesis in different cell lines, HeLa, tsA201, Jurkat, THP-1 and NIH/3T3 cells were infected with SIN-VSVG-MLV at a MOI of 2. Cells were lysed after different time intervals. The cytoplasmic fraction was recovered, and both products were purified and measured by quantitative PCR, using primers specifically designed to amplify ERT or LRT. The maximum amounts observed in each cell line were compared. As shown in Fig. 2A, the highest relative amounts of ERT were found in HeLa and tsA201 cells infected with SIN-VSVG-MLV (42,000 and 32,000 relative units, respectively). The amounts of ERT in NIH/3T3, Jurkat and THP-1 cells, on the other hand, were below 6000 relative units. The difference between HeLa and THP-1 cells was almost 140-fold. Consistent with this data, we observed similar results when relative amounts of LRT product were quantified (Fig. 2B). Again, the largest relative amount of product was found in HeLa cells (32,000 relative units), followed by tsA201 cells (11,000 relative units). We also detected a relatively small amount of LRT product in NIH/3T3, Jurkat and THP-1 cells (less than 300 relative units) as compared HeLa cells. The difference in LRT product between HeLa and THP-1 cells was almost 300-fold. These results suggest that the internalization efficiency of SIN-VSVG-MLV is higher in HeLa and tsA201 cells than in NIH/3T3, Jurkat and THP-1 cells.

Then, to compare the efficiency of LRT or viral DNA synthesis at different times, HeLa, tsA201, Jurkat, THP-1 and NIH/3T3 cells were infected with SIN-VSVGG-MLV at a MOI of 2. Cells were lysed at 6, 8, 16 and 24 h post infection (hpi). The cytoplasmic fraction was recovered, and the LRT product was purified and measured by quantitative PCR, using primers to amplify the LRT product. As shown in Fig. 3, peak LRT synthesis occurred at 6–8 hpi in HeLa (3A), tsA201 (3B) and Jurkat cells (3D) and at 16 hpi in THP-1 (3C) and NIH/3T3 cells (3E).

3.3. SIN-VSVG-MLV reverse transcription is approximately 85% in HeLa cells

The differential rates of vDNA synthesis observed in the various cell lines transduced with SIN-VSVG-MLV may be attributable to cellular factors present in some cell lines but not others, which may stabilize or favor RTC formation. To test this hypothesis, we analyzed RT efficiency, expressed as the percentage of LTR product generated relative to ERT product (Fig. 4). We found that when SIN-VSVG-MLV was transduced in HeLa cells, RT efficiency was approximately 70%, 66% and 85% at 2, 6 and 8 hpi respectively. In contrast, RT efficiency in tsA201, NIH/3T3, Jurkat and THP-1 cells was about 30% at these intervals (Fig. 4). At 16 and 24 h post-transduction, there were no significant differences in SIN-VSVG-MLV reverse transcription efficiency between cells lines. Taken together, our data suggest that the high levels of SIN-VSVG-MLV transduction observed in the HeLa cell line may be attributable to a significantly greater viral entry and RT efficiency. However, RT efficiency cannot explain the high levels of transduction in the tsA201 line, as these cells showed a RT efficiency of only 30%.

3.4. HeLa and tsA201 cells transduced with SIN-VSVG-MLV showed high levels of viral integration

Next, we analyzed SIN-VSVG-MLV integration into the host chromosomes of various cells, using a two-step *Alu*-based nested PCR assay. The NIH/3T3 cell line was excluded from analysis due to the large class of retrovirus-like elements in the mouse genome. Quantitative analysis showed significantly higher levels of viral integration in HeLa and tsA201 cells than Jurkat and THP-1 cells after transduction with SIN-VSVG-MLV (Fig. 5). However, integration does not seem to be a limiting step that might explain the differences in SIN-VSVG-MLV transduction in the cell lines analyzed.

3.5. SIN-VSVG-MLV transduction may be related to internalized virus levels and availability of the VSVG entry pathway

Since VSVG requires the LDL receptor (LDL-R) for cell entry, we analyzed the expression of this receptor in each cell lines. However, we

observed that LDL-R is present in a variable percentage of cells and its expression is not related to the level of transduction of SIN-VSVG-MLV (Fig. 6). Therefore, the availability of the receptor should not limit the transduction of SIN-VSVG-MLV.

The vesicular stomatitis virus has been reported to enter the cell via clathrin-mediated endocytosis (Sun et al., 2005). Therefore, we evaluated this pathway in all five cell lines, using a transferrin uptake assay that has been shown to rely on clathrin-mediated endocytosis (Kirchhausen et al., 2008). As shown in Fig. 7A and B, uptake of Transferrin Alexa Fluor 633 was highest in HeLa cells, followed by tsA201 cells, and lower in the other 3 cell lines. These results are consistent with the transduction levels observed in Fig. 1, suggesting a correlation between transduction efficiency and transferrin uptake.

To verify that SIN-VSVG-MLV entry is related to clathrin-mediated endocytosis, we used an inhibitor of this pathway, chlorpromazine. We observed a 70% and 83.2% decrease in SIN-VSVG-MLV transduction in HeLa and tsA201 cells, respectively (Fig. 7C). The effect of this inhibitor on the other cell lines could not be analyzed, due to low baseline rates of transduction and transferrin uptake.

These results suggest that SIN-VSVG-MLV enters cells via clathrin-mediated endocytosis and that differences in transduction levels observed are attributable to the relative availability of the pathway in each cell line.

4. Discussion

Self-inactivating murine leukemia virus-based vectors have been used for gene therapy due to a lower capacity for oncogene activation mediated by the U3 promoter region. El Ashkar and colleagues also generated a BinMLV vector that partially prevented the integrase from binding with the bromodomain and extra-terminal (BET) family of proteins as well as integration near oncogenes (El Ashkar et al., 2014). Development of new retroviral-derived vectors remains an active topic of research (El Ashkar et al., 2017). Pseudotyped MLV vectors have been used in gene therapy, cell and molecular biology applications and production of stable cell lines, and VSVG has been widely used for MLV pseudotyping. Although VSVG-pseudotyped vectors could be expected to show generally high transduction rates given the wide cellular tropism of VSV, we observed strong differences in transduction efficiency in several cell lines.

As such, HeLa cells presented the highest viral transduction efficiency, followed by tsA201 cells. Transduction efficiency in HeLa cells was almost 3-fold higher than in tsA201 cells and 6- to 7-fold higher than NIH/3T3, Jurkat or THP-1 cells (Fig. 1). To explain our results, we analyzed the steps of SIN-VSVG-MLV replication in each cell line, from ERT product synthesis to LRT product synthesis and integration, and then assessed vector entry into the various cell types.

Our results showed a relationship between vector transduction efficiency (Fig. 1) and relative amount of ERT and LRT product (Fig. 2) in a given cell line; high transduction efficiency was associated with highr relative amounts of both RT products. Strong-stop synthesis is independent of cellular factors and only the reverse transcriptase enzyme is necessary for its production. Therefore, ERT product can be used to quantify intracellular viral genomic RNA. On the other hand, cellular factors are crucial for successful DNA synthesis during LRT. In fact, Warrilow and colleagues observed that the presence of cellular factors significantly elevated HIV-1 LRT product synthesis *in vitro* by improving DNA elongation (Warrilow et al., 2010). When we analyzed RT by comparing the amounts of ERT and LRT product, we observed that SIN-VSVG-MLV transduction strongly stimulated LRT product synthesis in HeLa cells, consistent with the reverse transcription efficiency of up to 85% observed in this cell line. RT efficiency was only about 30% in the other cell lines (Fig. 4); in other words, RT efficiency was almost 3-fold higher in the HeLa line as compared to the other cells analyzed. Taken together, these results suggest that genomic viral RNA enters HeLa cells, and, to a lesser extent, tsA201 cells, in a highly efficient manner. We

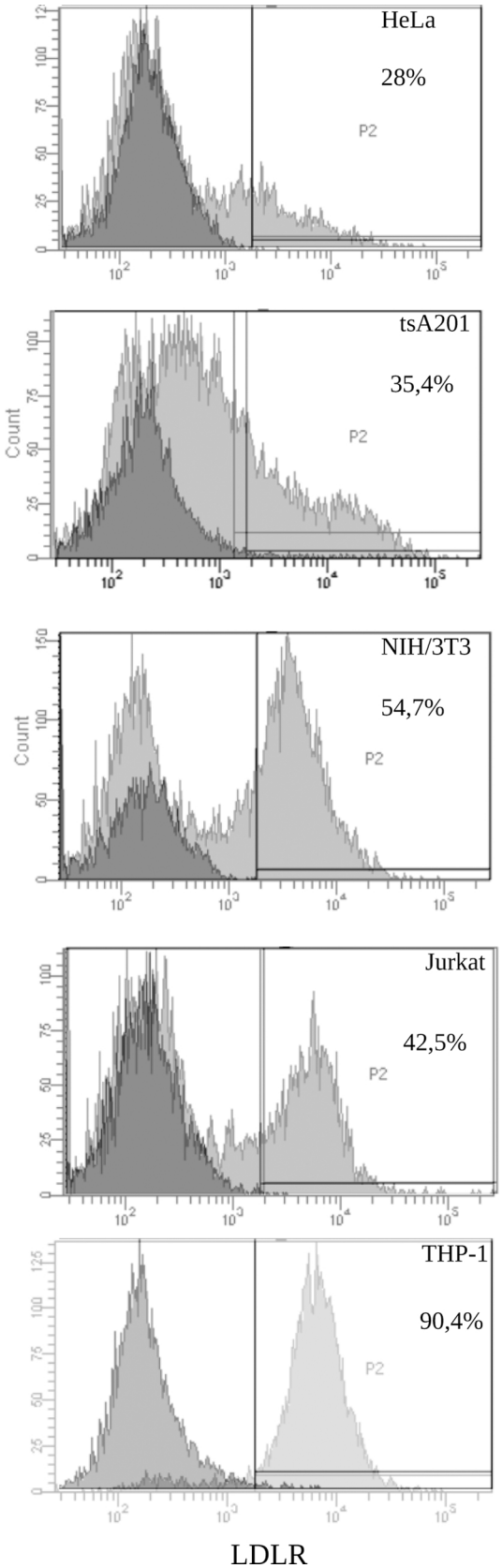

Fig. 6. Expression of LDL receptor on HeLa, tsA201, NIH/3T3, Jurkat and THP-1 cells. The cells were incubated with the anti-LDL receptor antibody followed by staining with anti-rabbit Alexa 488 antibody (light gray filled histogram), a control incubation with the latter antibody alone was performed (dark gray filled histogram) and analyzed by flow cytometry.

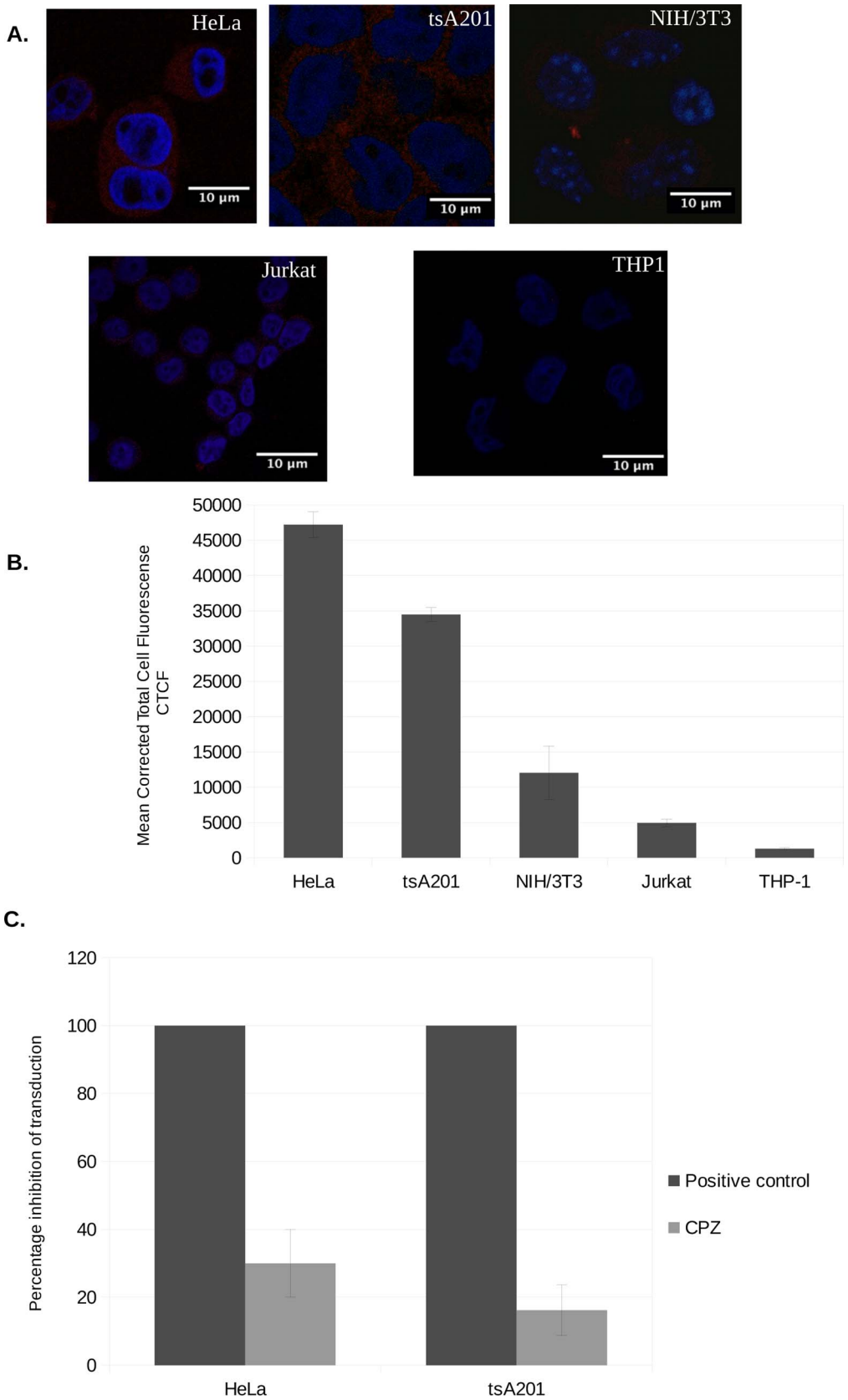

Fig. 7. Clathrin-mediated endocytosis in HeLa, tsA201, NIH/3T3, Jurkat and THP-1 cells. (A) Capture assay was performed using Transferrin Alexa Fluor 633 to assess clathrin-mediated endocytosis in HeLa, tsA201, NIH/3T3, Jurkat and THP-1 cells. **(B)** The corrected total cell fluorescence (CTCF) was calculated using ImageJ software. **(C)** Chlorpromazine (CPZ), an inhibitor of clathrin-mediated endocytosis, was used for this experiment. Cells were infected with SIN-VSVG-MLV for three days and analyzed by flow cytometry. Experiments were performed in triplicate. Graphs represent the average inhibition of SIN-VSVG-MLV transduction and the bars show the standard deviations.

also analyzed the kinetics formation of the LRT product. The timing of peak LRT product synthesis also varied between cell types, ranging from 6 to 16 hpi (Fig. 3). This and previous results suggest that the intracellular environment influences both the efficiency and the timing of vDNA synthesis. For instance, formation of the RTC and pre-integration complexes is affected by the availability of cellular proteins and nucleotides, intracellular traffic and other factors that may be cell type specific.

When we analyzed viral integration, we observed again that SIN-VSVG-MLV integration was higher in the HeLa line than in the other cells used in this study. This finding is likely due to high RT efficiency but also to a favored assembly of the pre-integration complex. Moreover, SIN-VSVG-MLV integration was also intermediately perceptible in tsA201 cells (Fig. 5), despite the low RT efficiency observed in this line. These findings suggest that once RT ends, the cell favors the formation and/or stability of the PIC and consequently viral integration.

Although RT of SIN-VSVG-MLV was more efficient in HeLa cells than in other cell types, this result alone cannot explain the differences in transduction efficiency observed; while transduction efficiency was also high in tsA201 cells, RT efficiency was low, similar to the levels observed in Jurkat, THP-1 and NIH/3T3 cells. In tsA201 cells, ERT product and transduction levels were correlated, suggesting that the vector genome was able to enter the cell efficiently. Therefore, we speculated that viral entry may be a limiting factor, which could explain the differences observed. SIN-VSVG-MLV recognizes the LDL receptor, which is ubiquitously expressed in human and mouse cells, and the 5 cell lines analyzed were all recognized by an anti-LDL antibody (Fig. 6). Therefore, we analyzed vector entry in each cell line, finding that HeLa and tsA201 cells showed high uptake of transferrin (Fig. 7), which enters the cell via clathrin-mediated endocytosis. Inhibition of this entry pathway resulted in decreased SIN-VSVG-MLV transduction (Fig. 7c). These results suggest that SIN-VSVG-MLV enters the cell via clathrin-mediated endocytosis and that the availability of this mechanism is a critical limiting factor in transduction of VSVG-pseudotyped MLV vectors.

5. Conclusions

Early SIN-VSVG-MLV replication events occurred with the highest efficiency in HeLa cells, followed by tsA201 cells and then Jurkat, THP-1 and NIH/3T3 cells. This differential transduction efficiency seems to be largely attributable to the relative availability of the entry mechanisms responsible for SIN-VSVG-MLV internalization and, to a lesser extent, the comparative efficiency of reverse transcription. Our results may help to elucidate virus-host interactions and facilitate selection of the optimal glycoprotein for MLV pseudotyping in various applications.

Funding

The research for this paper was financially supported by Fondecyt Grant 11121411 and U-Inicia Grant 11/08 to MA and Fondecyt Grant 1151250 to OL.

Conflict of interest

The authors confirm that there are no conflicts of interest associated with this publication.

Acknowledgements

The authors gratefully acknowledge to Johanna Saldias, Joseline Catrileo and Rosa Corvalán for their technical assistance.

References

Bruce, J.W., Bradley, K.A., Ahlquist, P., Young, J.A., 2005. Isolation of cell lines that show novel, murine leukemia virus-specific blocks to early steps of retroviral replication. J. Virol. 79, 12969–12978 https://doi.org/79/20/12969 [pii]r10.1128/JVI.79.20.12969-12978.2005.

Brussel, A., Sonigo, P., 2003. Analysis of early human immunodeficiency virus type 1 DNA synthesis by use of a new sensitive assay for quantifying integrated provirus. J. Virol. 77, 10119–10124.

Butler, S.L., Hansen, M.S.T., Bushman, F.D., 2001. A quantitative assay for HIV DNA integration in vivo. Nat. Med. 7, 631–634. http://dx.doi.org/10.1038/87979.

Cavazza, A., Cocchiarella, F., Bartholomae, C., Schmidt, M., Pincelli, C., Larcher, F., Mavilio, F., 2013. Self-inactivating MLV vectors have a reduced genotoxic profile in human epidermal keratinocytes. Gene Ther. 20, 949–957. http://dx.doi.org/10.1038/gt.2013.18.

Craigie, R., Bushman, F., Engelman, A., 1991. A rapid in vitro assay for HIV DNA integration. Nucleic Acids Res. 19, 2729–2734.

Duvillard, L., Florentin, E., Lizard, G., Petit, J.-M., Galland, F., Monier, S., Gambert, P., Vergès, B., 2003. Cell surface expression of LDL receptor is decreased in type 2 diabetic patients and is normalized by insulin therapy. Diabetes Care 26, 1540–1544.

El Ashkar, S., De Rijck, J., Demeulemeester, J., Vets, S., Madlala, P., Cermakova, K., Debyser, Z., Gijsbers, R., 2014. BET-independent MLV-based vectors target away from promoters and regulatory elements. Mol. Ther. Nucleic Acids 3, e179. http://dx.doi.org/10.1038/mtna.2014.33.

El Ashkar, S., Van Looveren, D., Schenk, F., Vranckx, L.S., Demeulemeester, J., De Rijck, J., Debyser, Z., Modlich, U., Gijsbers, R., 2017. Engineering next-generation BET-independent MLV vectors for safer Gene therapy. Mol. Ther. - Nucleic Acids 7, 231–245. http://dx.doi.org/10.1016/j.omtn.2017.04.002.

Elis, E., Ehrlich, M., Prizan-Ravid, A., Laham-Karam, N., Bacharach, E., 2012. p12 tethers the murine leukemia virus pre-integration complex to mitotic chromosomes. PLoS Pathog. 8, e1003103. http://dx.doi.org/10.1371/journal.ppat.1003103.

Finkelshtein, D., Werman, A., Novick, D., Barak, S., Rubinstein, M., 2013. LDL receptor and its family members serve as the cellular receptors for vesicular stomatitis virus. Proc. Natl. Acad. Sci. U. S. A. 110, 7306–7311. http://dx.doi.org/10.1073/pnas.1214441110.

Hacein-Bey-Abina, S., Pai, S.-Y., Gaspar, H.B., Armant, M., Berry, C.C., Blanche, S., Bleesing, J., Blondeau, J., de Boer, H., Buckland, K.F., Caccavelli, L., Cros, G., De Oliveira, S., Fernández, K.S., Guo, D., Harris, C.E., Hopkins, G., Lehmann, L.E., Lim, A., London, W.B., van der Loo, J.C.M., Malani, N., Male, F., Malik, P., Marinovic, M.A., McNicol, A.-M., Moshous, D., Neven, B., Oleastro, M., Picard, C., Ritz, J., Rivat, C., Schambach, A., Shaw, K.L., Sherman, E.A., Silberstein, L.E., Six, E., Touzot, F., Tsytsykova, A., Xu-Bayford, J., Baum, C., Bushman, F.D., Fischer, A., Kohn, D.B., Filipovich, A.H., Notarangelo, L.D., Cavazzana, M., Williams, D.A., Thrasher, A.J., 2014. A modified γ-retrovirus vector for X-linked severe combined immunodeficiency. N. Engl. J. Med. 371, 1407–1417. http://dx.doi.org/10.1056/NEJMoa1404588.

Hare, D., Collins, S., Cuddington, B., Mossman, K., 2016. The importance of physiologically relevant cell lines for studying virus–host interactions. Viruses 8, 297. http://dx.doi.org/10.3390/v8110297.

Ivaturi, S., Wooten, C.J., Nguyen, M.D., Ness, G.C., Lopez, D., 2014. Distribution of the LDL receptor within clathrin-coated pits and caveolae in rat and human liver. Biochem. Biophys. Res. Commun. 445, 422–427. http://dx.doi.org/10.1016/j.bbrc.2014.02.019.

Kirchhausen, T., Macia, E., Pelish, H.E., 2008. Use of dynasore, the small molecule inhibitor of dynamin, in the regulation of endocytosis. Methods Enzymol. 438, 77–93. http://dx.doi.org/10.1016/S0076-6879(07)38006-3.

Kohno, T., Mohan, S., Goto, T., Morita, C., Nakano, T., Hong, W., Sangco, J.C.E., Morimatsu, S., Sano, K., 2002. A new improved method for the concentration of HIV-1 infective particles. J. Virol. Methods 106, 167–173.

Lech, P., Somia, N.V., 2007. Isolation and characterization of human cells resistant to retrovirus infection. Retrovirology 4 (45). http://dx.doi.org/10.1186/1742-4690-4-45.

Livak, K.J., Schmittgen, T.D., 2001. Analysis of relative gene expression data using real-time quantitative PCR and the 2(-delta delta C(T)) method. Methods 25, 402–408. http://dx.doi.org/10.1006/meth.2001.1262.

Peng, K., Muranyi, W., Glass, B., Laketa, V., Yant, S.R., Tsai, L., Cihlar, T., Müller, B., Kräusslich, H.-G., 2014. Quantitative microscopy of functional HIV post-entry complexes reveals association of replication with the viral capsid. Elife 3, e04114. http://dx.doi.org/10.7554/eLife.04114.

Santos, S., Obukhov, Y., Nekhai, S., Bukrinsky, M., Iordanskiy, S., 2012. Virus-producing cells determine the host protein profiles of HIV-1 virion cores. Retrovirology 9 (65). http://dx.doi.org/10.1186/1742-4690-9-65.

Schambach, A., Mueller, D., Galla, M., Verstegen, M.M.A., Wagemaker, G., Loew, R., Baum, C., Bohne, J., 2006. Overcoming promoter competition in packaging cells improves production of self-inactivating retroviral vectors. Gene Ther. 13, 1524–1533. http://dx.doi.org/10.1038/sj.gt.3302807.

Schneider, W.M., Brzezinski, J.D., Aiyer, S., Malani, N., Gyuricza, M., Bushman, F.D., Roth, M.J., 2013. Viral DNA tethering domains complement replication-defective mutations in the p12 protein of MuLV gag. Proc. Natl. Acad. Sci. U. S. A. 110, 9487–9492. http://dx.doi.org/10.1073/pnas.1221736110.

Schweitzer, C.J., Jagadish, T., Haverland, N., Ciborowski, P., Belshan, M., 2013. Proteomic analysis of early HIV-1 nucleoprotein complexes. J. Proteome Res. 12, 559–572. http://dx.doi.org/10.1021/pr300869h.

Serhan, F., Jourdan, N., Saleun, S., Moullier, P., Duisit, G., 2002. Characterization of producer cell-dependent restriction of murine leukemia virus replication. J. Virol. 76,

6609–6617.
Sun, X., Yau, V.K., Briggs, B.J., Whittaker, G.R., 2005. Role of clathrin-mediated endocytosis during vesicular stomatitis virus entry into host cells. Virology 338, 53–60. http://dx.doi.org/10.1016/j.virol.2005.05.006.
Thornhill, S.I., Schambach, A., Howe, S.J., Ulaganathan, M., Grassman, E., Williams, D., Schiedlmeier, B., Sebire, N.J., Gaspar, H.B., Kinnon, C., Baum, C., Thrasher, A.J., 2008. Self-inactivating gammaretroviral vectors for gene therapy of X-linked severe combined immunodeficiency. Mol. Ther. 16, 590–598. http://dx.doi.org/10.1038/sj.mt.6300393.
Tiscornia, G., Singer, O., Verma, I.M., 2006. Production and purification of lentiviral vectors. Nat. Protoc. 1, 241–245. http://dx.doi.org/10.1038/nprot.2006.37.
Van Beveren, C., Goddard, J.G., Berns, A., Verma, I.M., 1980. Structure of moloney murine leukemia viral DNA: nucleotide sequence of the 5' long terminal repeat and adjacent cellular sequences. Proc. Natl. Acad. Sci. U. S. A. 77, 3307–3311.
Warrilow, D., Warren, K., Harrich, D., 2010. Strand transfer and elongation of HIV-1 reverse transcription is facilitated by cell factors in vitro. PLoS One 5, e13229. http://dx.doi.org/10.1371/journal.pone.0013229.
Willnow, T.E., 1999. The low-density lipoprotein receptor gene family: multiple roles in lipid metabolism. J. Mol. Med. (Berl.) 77, 306–315.